Available online at www.sciencedirect.com

ScienceDirect

IFAC PapersOnline CONFERENCE PAPER ARCHIVE

IFAC PapersOnLine 51-24 (2018) 1119–1126

Active Fault Tolerant Control of a Wind Farm System ⋆

Silvio Simani * **Cihan Turhan** **

* *Department of Engineering, University of Ferrara, Ferrara (FE) 44122 Italy (e–mail: silvio.simani@unife.it).*

** *Mechanical Engineering, Izmir Institute of Technology, 35430 Izmir, Turkey (e–mail: cihanturhan@iyte.edu.tr)*

Abstract: In order to enhance the 'sustainability' of offshore wind farms, thus skipping unplanned maintenance operations and costs, that can be important for offshore systems, the earlier management of faults represents the key point. Therefore, this work studies the development of an adaptive sustainable control scheme with application to a wind farm benchmark consisting of nine wind turbine systems. They are described via their nonlinear models, as well as the wind and wake effects among the wind turbines of the wind park. The fault tolerant control strategy uses the recursive estimation of the faults provided by nonlinear estimators designed via a nonlinear differential algebraic tool. This aspect of the study, together with the more straightforward solution based on a data–driven scheme, is the key issue when on–line applications are proposed for a viable implementation of the proposed solutions.

Keywords: Fault reconstruction, sustainable control, nonlinear model, robustness and reliability, offshore wind farm.

1. INTRODUCTION

Generally, wind turbines of important size can be quite expensive, and thus their reliability cannot be neglected in order to optimise their energy conversion rate and minimise the lost production costs. This point could represent the key point for offshore wind parks, where Operation and Maintenance (O & M) related activities have to be reduced, since they directly affect the final energy price. The so–called cost of the capital, and the wind turbine load carrying structure of the installations constitute the main term in the price of the energy, which represents its 'fixed cost'. On the other hand, the O & M term is a 'variable cost' that affect the cost up to the 30% (Simani and Farsoni (2018)).

In parallel, industrial plants became more and more complex with increased price, which can barely tolerate any performance reduction to faults and disturbance, thus leading to the decrease of the production and process safety. This also yields to require increased levels of reliability and safety for the control systems, as they can be subjected to system anomalities and failures. Therefore, it is really necessary the Fault Detection and Diagnosis (FDD) task or the Fault Detection and Isolation (FDI) phase, as well as the requirement of sustainable (*i.e.* fault–tolerant features) for reducing any possible performance reduction, thus avoiding any anomalous and dangerous situations. Therefore, this paper tries to propose the design of sustainable, *i.e.* a Fault Tolerant Control (FTC) system, with an application example to a wind park simulation model.

Quite recently, several works have been suggested for wind turbine FDI/FDD, and the most important are recalled *e.g.* in (Odgaard et al. (2013)). In the same way, with reference to the sustainable (FTC) problem, it was quite recently considered but for an offshore wind turbine simulated model in (Odgaard et al. (2013)). Generally, sustainable (FTC) strategies are divided into two schemes, *i.e.* Passive Fault Tolerant Control Strategies (PFTCS) and Active Fault Tolerant Control Strategies (AFTCS), as summarised *e.g.* in (Simani and Farsoni (2018)).

With particular reference to wind parks, sustainable control strategies were considered *e.g.* in (Odgaard and Stoustrup (2013)). These plants have complex and nonlinear dynamic behaviours, due to their aerodynamics that are nonlinear and unsteady. Moreover, their rotors are affected by complex and turbulent wind fields and driven by extreme fatigue loading conditions. Therefore, the compensation of wind parks can require complex and challenging design strategies, as described *e.g.* in (Simani and Farsoni (2018)).

In particular, this work considers the design of an active sustainable control scheme (*i.e.* an AFTCS) that includes a reliable fault reconstruction strategy with the development of a controller accommodation methodology. In more detail, the strategy uses a recursive fault reconstruction provided by nonlinear fault estimators achieved with the so–called NonLinear Geometric Approach (NLGA) tool, a nonlinear differential algebraic method already proposed by the authors in (Simani and Castaldi (2014)). It is worth noting that the nonlinear fault reconstruction scheme relies on the NLGA tool addressed at the beginning *e.g.* in (Simani and Castaldi (2014)). However, it is not able to provide any fault size estimation, which is strictly required

⋆ Invited paper for the special session on 'Fault Tolerant Control of Wind Turbines' organised by Ron J. Patton and Silvio Simani.

10.1016/j.ifacol.2018.09.728

for this application. Moreover, the straightforward use of the proposed scheme, or any other method exploiting the *analytical* disturbance decoupling approach, would be impossible, mainly due to the wind park model formulation and its structure. In fact, the wind turbine aerodynamic models are nonlinear functions of the tip–speed ratio and blade pitch angle (Simani and Castaldi (2018)).

The interactions among the wind turbines of the wind park are regarded as a disturbance terms, since, followed by the wind model, they reduce the performances of the control scheme. Note that different FDI/FDD solutions, which also enhance the features the same wind park, were recently used with application to the same wind park challenge competition, as summarised in in (Simani and Farsoni (2018)). It is worth noting also that the active nonlinear filters and the sustainable control strategy are applied to the wind farm benchmark simulator proposed in (Odgaard and Stoustrup (2013)), in the presence of faults and model–reality mismatch conditions. A similar FTC solution proposed for the same benchmark but relying on fuzzy logic tools was addressed in (Simani et al. (2018)). Therefore, the development of the sustainable active strategy for the wind farm benchmark and relying on nonlinear fault reconstructors are the novel aspects of this contribution. According to the requirements highlighted in (Odgaard and Stoustrup (2013)), this work assumes that the proposed approach has been applied to the whole wind park, considered as distributed system, and not separately to each wind turbine.

Moreover, the developed solution are compared with respect to the former techniques designed by the same authors *e.g.* in (Simani and Farsoni (2018)). On one hand, the strategy described in this work uses adaptive fault reconstructors that are able to counteract in an recursive way any fault situations. On the other hand, the strategy relying on the fuzzy logic tool is obtained in a batch way, in order to compensate in a passive way all the possible fault situations regarding the controlled process, thus being a PFTCS solution.

Finally, it is worth observing that this work tries to generalise the solutions proposed by the same authors *e.g.* in (Simani and Castaldi (2017)), and it compares the achievements already addressed by the same authors in (Simani and Farsoni (2018)).

The paper has the following organisation. Section 2 describes the wind farm benchmark. Section 3 addresses the fault reconstruction scheme, as well as the design of the sustainable control strategy, which represents the main structure of the AFTCS solution. The obtained results are summarised and discussed in Section 4, where comparisons with respect to different sustainable control schemes are also presented. Finally, Section 5 ends the paper by highlighting the main points of the paper, and it suggests open problems and future issues that could require further investigations.

2. WIND FARM SIMULATOR

The application benchmark consists of a small wind park of 9 wind turbines located in a coordinate system of a square matrix 3×3, as explained in (Odgaard and Stoustrup (2013)). The distance between 2 wind turbines in both directions is $7\,L$, where L represents the wind turbine rotor diameter. 2 measuring devices (masts) are placed in front of the wind turbines, and located in each of the 2 wind directions, *i.e.* 0^o and 45^o. These masts, which provide a measurement of the wind speed, are located $10\,L$ in front of the wind park, in order to avoid the effect of the wind park wakes. The wind turbines of the wind park are generic 4.8 MW systems described in (Odgaard et al. (2013)). They are three bladed horizontal axis, pitch controlled variable speed wind turbines, that are described in detail in (Odgaard and Stoustrup (2013)).

The i–th wind turbine system is represented as a dynamic model that includes control logics, variable parameters and 3 state variables. Therefore, the i–th wind turbine model produces the electrical power $P_{i\,g}(t)$, is controlled by the collective pitch angle $\beta_i(t)$, and the generator speed $\omega_{i\,g}(t)$. For each turbine, only one measured pitch angle β_i is exploited as the i–th wind turbine controller regulates the pitch angles in the same way (Odgaard and Stoustrup (2013)).

2 different wind distribution scenarios are considered for each direction of 0^o and 45^o, but the wind park is driven by the same wind process $v_w(t)$, and possibly affected by a time shift. The considered wind process contains a wind sequence with a mean speed value increasing from 5 m/s to 15 m/s, and with possible maximum peaks of about 23 m/s.

The simulated benchmark considered in this work contains a simple wind farm controller that regulates the power reference $P_{i\,ref}(t)$. If the generated power is lower than the one requested, the reference signals $P_{i\,ref}(t)$ are evenly distributed among the different wind turbine controllers. More details regarding this wind park benchmark, whose description is beyond the scope of this work, are addressed in (Odgaard and Stoustrup (2013)). It is worth observing that the description of the considered wind park could be quite simple. However, the benchmark is able to accurately represent realistic wind park systems.

The simulated benchmark is composed of three blocks. The wake description is recalled in the following, as addressed in (Odgaard and Stoustrup (2013)). It provides the mathematical formulation of the wind distribution among the wind turbines of the park, thus representing the interactions among the different wind turbines and their wakes. This wakes distribution is a function of the different control laws, so that up–wind turbines can affect their wakes, thus increasing or decreasing the control actions of the down–wind turbines.

The wind park simulator model provides different signals that can be used for FTC purpose. In particular, v_w describes the wind speed vector, whose components are $v_{i,\,w}$. On the other hand, $v_{w,\,m}$ represents the wind speed vector provided by the masts, whose components are $v_{i,\,w,\,m}$. The variable P_r is the vector of the power references required by the i–th wind turbine of the wind park, $P_{i\,r}$. P_g is the vector containing the generated electrical powers with reference to the i–th wind turbine, $P_{i\,g}$. Finally, the signal β is the pitch angle vector for each wind turbine, controlled by the signal β_i, whilst ω_g is the generator speed vector

from the measured wind turbine velocities, $\omega_{i\,g}$. The wake distribution is described as the effect of a wind efficacy decrease between the wind turbines of a factor 0.9. On the other hand, the wind turbulence effect is modelled by random process of zero mean and variance of 0.2 (Odgaard and Stoustrup (2013)).

The overall model of the wind park under consideration has the form of Eq. (1):

$$\begin{cases} \dot{x}_c(t) = f_c\left(x_c(t), u(t)\right) \\ y(t) = x_c(t) \end{cases} \tag{1}$$

with $u(t) = [v_{i\,w}(t),\, v_{j\,w\,m}(t),\, P_{i\,r},\, \beta_i(t)]^T$ and $y(t) = x_c(t) = [\omega_{i\,g}(t),\, P_{i\,g}(t)]^T$ representing the input and the measured output signals, respectively. The subscript i indicates the generic i–th wind turbine of the wind park that is affected by the j–th wind wake effect, with $i,\, j = 1, \ldots, 9$, and $i \neq j$. $f_c(\cdot)$ is a continuous–time nonlinear function used to describe the nonlinear behaviour of the considered dynamic process. A number of N sampled data $u(k)$ and $y(k)$, with $k = 1,\, 2,\, \ldots\, N$, will be acquired from the system of Eq. (1). They will be used for deriving the mathematical models of the disturbance effects depending on both the wind process $v_w(t)$ by means of the nonlinear aerodynamic behaviour and the wind turbine wakes $v_{w,m}$ *i.e.* the wind turbine interactions, as described in Sections 3 and 4.

2.1 Fault Scenario

This wind park benchmark implements 3 fault cases that affect the wind turbine measurements, *i.e.* the signals $\beta_i(t)$, $\omega_{i\,g}(t)$, and $P_{i\,g}(t)$. It is worth noting that these fault conditions may be diagnosed by considering the overall wind park system, for example by comparing the different wind turbine performances; however, they are difficult to be detected by considering the single wind turbine models. Moreover, these fault cases regard different wind turbines at different time instants, as addressed in (Odgaard and Stoustrup (2013)).

Table 1 summarises the relations among the fault cases considered in the paper and the i–th wind turbine of the wind farm. Section 3 will exploit this analysis and will show how the disturbance decoupling method proposed in this work is able to improve the fault diagnosis stage, thus employed for the controller compensation task. This aspect highlights the key point of the contribution of this paper.

Table 1. Fault cases of the wind farm simulator.

Fault case #	1	2	3
Faulty wind turbine i	2	1	6
	7	5	8

In this way, Table 1 represents the fault effects among the wind turbines, by considering the single fault case occurrence.

In particular, with reference to the rationale behind the fault scenario considered in this paper, the following remarks can be drawn. The fault case 1 is due to the debris build–up, *i.e.* the wind turbine blade dirt. This dirt modifies the aerodynamics law of the wind turbine model, usually by reducing the achieved power. The fault case 2 effect derives form a misalignment of the wind turbine blades installed during the installation stage of the wind park. This effect is modelled as offset between the measured signal and real pitch angle of one or more blades. This may induce also a dangerous mismatch between the blade loads, thus possibly exciting the dynamics modes of the load carrying structure. Finally, the fault case 3 is due to an alteration in the drive–train model parameters produced by wear and tear. A more detailed description of this fault scenario can be found *e.g.* in (Odgaard and Stoustrup (2013)).

The following of this section analyses the links among the different fault cases reported in Table 1 and their effects on the measurements acquired from the simulated model of Eq. (1). In order to describe a realistic scenario, this system is also affected by uncertainty, measurement errors and the well–known model–reality mismatch. This point is fundamental when the reliability and robustness features of the proposed solutions have to be analysed for the viable application of the suggested methodologies. In fact, Section 4 will demonstrate how the development of the nonlinear fault reconstructors for diagnosis purpose improves the sustainable strategy described in this paper. This is a key point of the proposed methodology.

In more detail, Table 2 reports the effects of the fault scenario on the input and output signals acquired from the wind farm benchmark model of Eq. (1). Moreover, these measured signals are used for the development of the nonlinear fault reconstructors addressed in Section 3 and validated in Section 4.

Table 2. Results of the failure mode & effect analysis for the wind farm model.

Fault case	1	2	3
u	$v_{2\,w}$, $v_{7\,w}$	$v_{1\,w}$, $v_{5\,w}$	$v_{6\,w}$, $v_{8\,w}$
	$v_{4\,w\,m}$, $v_{9\,w\,m}$	$v_{2\,w\,m}$, $v_{6\,w\,m}$	$v_{3\,w\,m}$, $v_{7\,w\,m}$
	$P_{2\,r}$, β_7	$P_{1\,r}$, β_2	$P_{6\,r}$, β_3
y	$\omega_{9\,g}$, $P_{4\,g}$	$\omega_{5\,g}$, $P_{6\,g}$	$\omega_{8\,g}$, $P_{7\,g}$

The results summarised in Table 2 were achieved by performing a fault sensitivity analysis, which represents an viable tool applied to dynamic processes, as described in (Simani and Farsoni (2018)). In practice, for each fault case, the measurements reported in Table 2 represent the most sensitive signals acquired from the model of Eq. (1) in the presence of the considered fault situations. Obviously, when a different fault scenario has to be analysed, different measurements should probably be considered. Moreover, even if it is assumed that the faults do not occur at the same time, this does not limit the validity of the proposed approach, as highlighted in (Simani and Farsoni (2018)). On the other hand, the fault can be diagnosed whatever their localisation.

Finally, it is worth noting that the disturbance decoupling procedure considered in this work and addressed in Section 3 represents the key contribution of this paper. The proposed methodology is fundamental since the disturbance and the uncertainty effects due to the interactions among the wind turbines of the wind farm can reduce the capabilities of the sustainable control scheme. In fact,

these disturbance terms can mask the effects of the fault conditions regarding the wind turbines, as highlighted in the following.

3. FAULT TOLERANT CONTROL DESIGN

The proposed sustainable control scheme is developed in 3 steps. The first stage concerns the identification of the mathematical description of the nonlinear disturbance terms, which are used for the development of the NLGA fault reconstructors. Thus, the estimated faults are employed for the compensation of both the measured and control signals affected by the faults themselves.

In order to obtain reliable and robust solutions, the disturbance terms affecting the model under diagnosis need to be cancelled out. Section 2 shown how these terms derive from 2 effects: one is due to the wind signal $v_{i\,w}$ regarding the i–th wind turbine system via its power coefficient factor C_p. The elimination of this term was already addressed by the same authors in (Simani and Castaldi (2014)) but developed only for a single wind turbine model. The same strategy will be exploited here and developed for the different wind turbines of the park; the second disturbance term is generated by the interactions among the wind turbine systems, and described by the wind signals $v_{j\,w\,m}(t)$ of the different wakes.

On one hand, in (Odgaard and Stoustrup (2012)) it was shown that the derivation and the cancellation of the first disturbance effect can rely on the analytical identification of both the C_p factor and the wind velocity $v_w(t)$. On the other hand, with reference to the wind wakes, a new methodology using the NLGA tool is proposed in this work. In more detail, by following the same strategy used for the cancellation of the uncertainty of wind speed $v_w(t)$ described in (Simani and Castaldi (2014)), this scheme needs for the nonlinear mathematical description of the disturbance distribution relation of the signals $v_{j\,w\,m}(t)$. Therefore, as described in (Simani and Castaldi (2014)), the function $C_p\,(\beta,\,\lambda)$ entering into the aerodynamic models of the wind turbines and included in Eq. (1) was obtained as a two–dimensional polynomial description. It depends on the tip–speed ratio λ and the blade pitch angles β of the i–th wind turbine system. The same strategy was used for removing the effect of the other inputs $v_{j\,w\,m}(t)$ by exploiting the identification procedure presented for the first time in (Simani and Castaldi (2014)).

Once the disturbance distribution term has been derived in mathematical form, the next step of the sustainable control scheme development requires the design of the nonlinear fault reconstructors for fault diagnosis purpose. Their models are achieved via the disturbance cancellation strategy originally traced back to the NLGA methodology (Simani and Castaldi (2014)). This procedure allows to design a coordinate transformation that highlights a subsystem depending only on the faults but insensitive to the disturbance signals, which represents the first step in the development of the fault reconstructors. Note that, in this way, the fault reconstructors do not depend on the disturbance d, that in this paper represent the vector $[v_{i\,w},\, v_{j\,w\,m}]$.

This scheme applies to the general nonlinear system of Eq. (2):

$$\begin{cases} \dot{x} \,=\, n(x) + g(x)\,c + \ell(x)\,f + p_d(x)\,d \\ y \,=\, h(x) \end{cases} \tag{2}$$

with $x \in \mathcal{X}$ is an open subset of $\mathbb{R}^{\ell_n}$, the signal $c(t) \in \mathbb{R}^{\ell_c}$ represents the input vector, the term $f(t) \in \mathbb{R}$ is the fault signal, whilst the vector $d(t) \in \mathbb{R}^{\ell_d}$ is the disturbance effect, and the vector $y \in \mathbb{R}^{\ell_m}$ is the system output. The nonlinear functions $n(x)$, $\ell(x)$, $g(x)$, and $p_d(x)$ are smooth vector fields, whilst $h(x)$ is a smooth map.

The derivation of the nonlinear fault reconstructors for the fault signal f that are decoupled from the disturbance d relies on the algorithm addressed in (Castaldi et al. (2010)). In that work the original NLGA scheme of (Simani and Castaldi (2014)) was modified to be applied to the FDI problem. By means of a suitable coordinate change, the model of Eq. (2) is transformed into a new system in the local coordinates $(\bar{x}, \bar{y})$ in the form of Eq. (3) (Castaldi et al. (2010)):

$$\begin{cases} \dot{\bar{x}}_1 \,=\, n_1(\bar{x}_1, \bar{x}_2) + g_1(\bar{x}_1, \bar{x}_2)\,c + \ell_1(\bar{x}_1, \bar{x}_2, \bar{x}_3)\,f \\ \dot{\bar{x}}_2 \,=\, n_2(\bar{x}_1, \bar{x}_2, \bar{x}_3) + g_2(\bar{x}_1, \bar{x}_2, \bar{x}_3)\,c + \\ \qquad +\ell_2(\bar{x}_1, \bar{x}_2, \bar{x}_3)\,f + p_2(\bar{x}_1, \bar{x}_2, \bar{x}_3)\,d \\ \dot{\bar{x}}_3 \,=\, n_3(\bar{x}_1, \bar{x}_2, \bar{x}_3) + g_3(\bar{x}_1, \bar{x}_2, \bar{x}_3)\,c + \\ \qquad +\ell_3(\bar{x}_1, \bar{x}_2, \bar{x}_3)\,f + p_3(\bar{x}_1, \bar{x}_2, \bar{x}_3)\,d \\ \bar{y}_1 \,=\, h(\bar{x}_1) \\ \bar{y}_2 \,=\, \bar{x}_2 \end{cases} \tag{3}$$

where $\ell_1(\bar{x}_1, \bar{x}_2, \bar{x}_3)$ is not identically zero. The system of Eq. (3), when this transformation exists, is observable. Moreover, the subsystem $\bar{x}_1$, which depends on f and insensitive to the disturbances d, will be used for the design of the fault reconstructors (Castaldi et al. (2010)).

The feasibility of this transformation depends on some fault detectability conditions, that need to be satisfied, as remarked in (Castaldi et al. (2010)). Moreover, the system of Eq. (2) consists of 3 submodels of Eqs. (3), where this $\bar{x}_1$–subsystem is always insensitive to the disturbance effects d, but depending on the fault signals f, as highlighted by the relation of Eq. (4):

$$\begin{cases} \dot{\bar{x}}_1 \,=\, n_1(\bar{x}_1, \bar{y}_2) + g_1(\bar{x}_1, \bar{y}_2)\,c + \ell_1(\bar{x}_1, \bar{y}_2, \bar{x}_3)\,f \\ \bar{y}_1 \,=\, h(\bar{x}_1) \end{cases} \tag{4}$$

where the state vector $\bar{x}_2$ in Eq. (3) can be measured, whilst $\bar{x}_2$ in Eq. (4) is an exogenous input, that is indicated as $\bar{y}_2$.

The developed nonlinear fault reconstructors obtained via the modified NLGA tool implement the least–squares algorithm with forgetting factor, which rely on the adaptation law of Eqs. (5):

$$\begin{cases} \dot{P} \,=\, \beta\,P - \dfrac{1}{N^2} P^2 \breve{M}_1^2, & P\,(0) = P_0 > 0 \\ \dot{\hat{f}} \,=\, P\,\epsilon\,\breve{M}_1, & \hat{f}\,(0) = 0 \end{cases} \tag{5}$$

where the Eq. (6) is the estimation of the output signal, whilst the corresponding normalised estimation error has the form of Eq. (6):

$$\begin{cases} \hat{\breve{y}}_{1s} \,=\, \breve{M}_1\,\hat{f} + \breve{M}_2 + \lambda\,\breve{\bar{y}}_{1s} \\ \epsilon \quad\,=\, \dfrac{1}{N^2}\left(\bar{y}_{1s} - \hat{\breve{y}}_{1s}\right) \end{cases} \tag{6}$$

Note that all the variables of the adaptive fault reconstructor of Eq. (6) are scalar. In particular, the variable $\lambda > 0$ is a parameter regarding the bandwidth of the filter. The variable $\beta \geq 0$ represents the forgetting factor, whilst $N^2 = 1 + \breve{M}_1^2$ describes the normalisation parameter of the least–squares method. Moreover, the developed fault reconstructor uses the input signals $\breve{M}_1$, $\breve{M}_2$, $\breve{\bar{y}}_{1s}$, that are achieved via a low–pass processing of the variables M_1, M_2, $\bar{y}_{1s}$ as described by Eqs. (7):

$$\begin{cases} \dot{\breve{M}}_1 = -\lambda \breve{M}_1 + M_1, \; \breve{M}_1(0) = 0 \\ \dot{\breve{M}}_2 = -\lambda \breve{M}_2 + M_2, \; \breve{M}_2(0) = 0 \\ \dot{\breve{\bar{y}}}_{1s} = -\lambda \breve{\bar{y}}_{1s} + \bar{y}_{1s}, \; \breve{\bar{y}}_{1s}(0) = 0 \end{cases} \tag{7}$$

The fault reconstructor systems are adaptive filters consisting of the relations of Eqs. (5), (6), and (7). Note also that the same authors in (Castaldi et al. (2010)) showed that this adaptive filter generates a signal $\hat{f}(t)$ that asymptotically approximates the real fault f. Moreover, these reconstructed faults can have general models, as remarked in (Simani and Farsoni (2018)). Note that this methodology is valid for the reconstruction of both actuator and sensor faults, as described in (Castaldi et al. (2017)).

Once the fault reconstructor block has been designed, these reconstructed fault signals can be exploited for the accommodation of the control signals P_g, β, and ω_g that are altered by the faults themselves of the wind park system. This step is the third stage in the development of the complete sustainable control strategy. Moreover, the simulation results of Section 4 will be obtained by considering the sustainable control scheme reported in Fig. 1. This scheme implements the wind park controller developed in (Odgaard and Stoustrup (2013)).

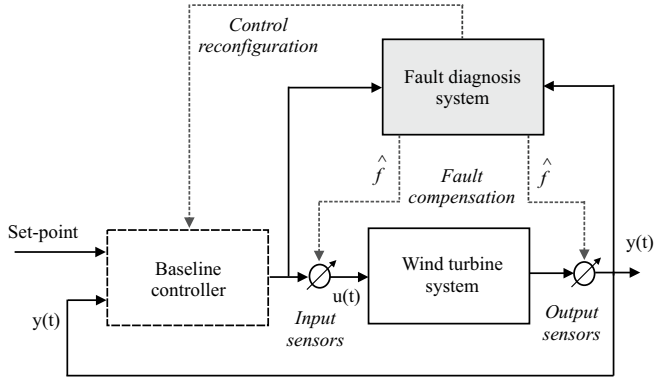

Fig. 1. The developed sustainable control scheme.

The complete scheme reported in Fig. 1 shows that the sustainable control scheme is implemented by integrating the fault reconstruction task with the existing control system. This fault reconstruction block (FDI) gives the reconstruction of the actuator and sensor faults $\hat{f}$, that are injected into the control loop. In this way, they are able to accommodate the effect of the faults themselves, that have modified the measured and controlled signals. After this compensation, the wind turbine controller is able to guarantee the nominal tracking of the reference signal, as for the nominal or fault–free case. Note that, according to the scheme of Fig. 1, the fault compensation mechanism is always acting in the control scheme, as the fault estimation is zero in the fault–free case. A switching logic is thus not required.

Finally, note that in steady–state conditions, once the fault effects are completely cancelled out, the performances of the control scheme coincide with the fault–free situation. Therefore, the stability issues of the sustainable control scheme have to be considered only during the transient phases, since the faults have not yet accommodated. In fact, during this phase, the reconstruction errors of the faults could destabilise the closed–loop system of Fig. 1. However, by following *e.g.* the demonstration presented in (Castaldi et al. (2014)), it is possible to demonstrate that the fault reconstruction error is limited and convergent to zero, and the stability of the overall closed–loop system is thus achieved.

4. SIMULATION RESULTS

This section summarises the development and the results achieved from the sustainable control scheme applied to the wind farm benchmark model. In more detail, the first part of this section describes the derivation of the disturbance distribution functions in Eq. (2).

In particular, the entries of the C_p–map of the wind turbine aerodynamic system has been described by means of 2–dimensional polynomial of Eq. (8):

$$\hat{C}_p(\lambda_i, \beta_i) = -0.0013\,\lambda_i^3 + 0.0003\,\lambda_i^3\,\beta_i + 0.010\,\lambda_i^2 \tag{8}$$

with reference to the i–th wind turbine system. More details on the procedure for achieving this polynomial were described in (Simani and Castaldi (2014)). In the same way used for the estimation of this term, the disturbance functions representing the $p_d(x)$ term of Eq. (2) and derived from the wind wakes are described as $\hat{C}_{p\,i}$ in Eq. (9):

$$\hat{C}_{p\,i}(\lambda_j, \beta_j) = -0.0011\,\lambda_j^2 + 0.0027\,\beta_j\,\lambda_j^2 \tag{9}$$

for the the j–th turbine wake affecting the i–th turbine of the farm.

Note that the proposed strategy allows to derive the mathematical formulation of the disturbance functions for all uncertainties, and not only due to the errors from the C_p entry variations and the interferences of the wind wakes among the wind turbines of the park. This remark is important since these terms are exploited for the derivation of the fault reconstruction filters, all uncertainty effects have to be taken into account. A similar method was described in (Simani et al. (2003)) but developed only for linear time–invariant systems. Therefore, the uncertainty distribution function $p_d(x)$ entering into the nonlinear system of Eq. (2) is obtained using the input–output data acquired from the wind farm. An important hypothesis that has to be valid in this situation is that the model–reality mismatch changes slower than the effects of the disturbance terms, *i.e.* the signals d in Eq. (2). Another important issue concerns the estimated function $p_d(x)$ regarding the uncertainty structure, that should be independent from the wind size represented by the signal d. This means that the so–called disturbance directions are

the most important feature of the disturbance decoupling approach proposed in this work.

In this way, the fault reconstruction adaptive filters of Eqs. (5), (6), and (7) developed via the NLGA tools generate the estimate of the different fault signals affecting the the wind park simulator, as shown in Section 2. The development of these fault reconstruction adaptive filters that are used for fault compensation is summarised in the following. More analytical details of the mathematical procedure are presented in (Simani and Castaldi (2014)) for the single wind turbine model. On the other hand, the implementation of the designed filters is detailed in (Simani and Farsoni (2018)).

When the model of Eq. (2) is defined, the following vectors are defined, with reference to the wind park benchmark: $x = [x_1\, x_2]^T = [\omega_{i\,g}\, P_{i\,g}]^T$, $c = [P_{i\,r}\, \beta_i]^T$, and the functions below are fixed:

$$n(x) = \left[-\frac{\rho\, A}{2\, J}\, 0.0010\, R^3\, x_1^2 - \frac{1}{J}\, x_2 \;\; -p_{gen}\, x_2 \right]^T \tag{10}$$

$$g(x) = \begin{bmatrix} 0 & \dfrac{\rho\, A}{2\, J}\, 0.0003\, R^3\, x_2^2 \\ p_{gen} & 0 \end{bmatrix} \tag{11}$$

and:

$$\ell(x) = \begin{bmatrix} 0 & \dfrac{\rho\, A}{2\, J}\, 0.0003\, R^3\, x_1^2 \\ 0 & 0.0001 \end{bmatrix} \tag{12}$$

for the i–th wind turbine. Note that the subscript i is dropped. Moreover, $p_d(x)$ has the following form:

$$p_d(x) = \begin{bmatrix} \dfrac{\rho\, A}{2\, J}\, 0.0010\, R^2\, x_1 & 0.0011 \\ 0.0002 & \dfrac{\rho\, A}{2\, J}\, 0.0027\, x_2 \end{bmatrix} \tag{13}$$

When the model of Eq. (1) is considered, taking into account Eqs. (2), (13), (12), and (11), it can be shown that:

$$S_0 = \bar{P} = \mathrm{cl}\left(p_d(x)\right) \equiv p_d(x) \tag{14}$$

Moreover, if $\ker\{dh\} = \emptyset$, it is easy to verify that $\Sigma_*^P = \bar{P}$ as $\bar{S}_0 \cap \ker\{dh\} = \emptyset$. Therefore, the expression $\left(\Sigma_*^P\right)^\perp = \left(\bar{P}\right)^\perp$ needs to be computed. However, note that for the system under diagnosis, the derivation of the observability codistribution $\left(\Sigma_*^P\right)^\perp = \left(\bar{P}\right)^\perp$ is improved by observing Eq. (14). More analytical details are similar to the results already addressed by the same authors for the case of the single wind turbine, and they will not be recalled here. The interested reader can refer to (Simani and Farsoni (2018)).

Finally, as an example, with reference to the fault case 2, the development of the nonlinear fault reconstruction adaptive filter that generates the estimation of the fault signal f affecting the actuator $\beta_i(t)$ has the form of Eq. (15):

$$\dot{\bar{y}}_{1s} = M_2 + M_1 \cdot f \tag{15}$$

with:

$$\begin{cases} M_1 \;=\; -0.0361\, x_1 + 0.8019\, x_1^2 \\ M_2 \;=\; 0.7754\, x_1^2 - 0.3347\, x_1^3 + 15.7897\, x_2 + 1.0234\, x_2^2 \end{cases} \tag{16}$$

On the other hand, the derivation of the fault reconstruction filters for the cases 1 and 3 is basically relying on a different choice of the vectors of Eq. (12), which lead to other forms for the nonlinear adaptive filter of Eq. (15). For example, with reference to the fault case 2 reported in Table 1, the nonlinear fault reconstruction filter insensitive to the disturbance effect d describing both the wind $v_w(t)$ and the wake $v_{w,\,m}$ terms is described by the model of Eq. (5). A proper selection of the adaptation parameters entering in Eqs. (5), (6), and (7), the nonlinear adaptive reconstructor generates a good approximation of the fault size, with minimal detection delay.

Therefore, the simulations reported in Figure 2 regard the case of the actuator fault f described as a sequence of 2 rectangular pulses affecting 2 turbines, as described in Section 2.1. In particular, Figure 2 reports the fault reconstruction (dashed black line), when compared with respect to a fixed threshold used for the FDI task (grey dotted line) and the real fault (dashed gray line).

The developed fault reconstruction adaptive filters not only allow for the fault detection and their isolation, but also the fault estimation. Moreover, the considered faults described as sequences of rectangular pulses have been included in the wind farm simulator, since they can describe actual fault situations with reference to the wind farm under investigation. However, as already highlighted, the fault reconstruction systems can be easily modified to provide, for example, the estimation of general signals, if the nonlinear adaptive filter design can include the fault internal models.

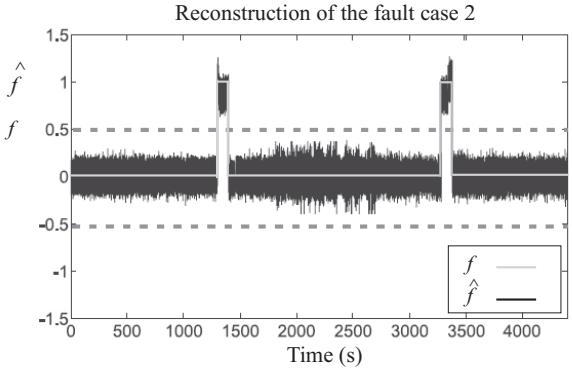

Fig. 2. Recursive reconstruction of the fault case 2.

Note finally that the analytic proof of the convergence and the stability of the proposed solutions can be derived by following the results already proposed by the authors in (Castaldi et al. (2014)).

4.1 Sensitivity Analysis and Comparisons

In order to highlight advantages and drawbacks of the proposed solutions, the features of the sustainable control scheme applied to the wind park benchmark were analysed with respect to the per–cent Normalised Sum of Squared Error ($NSSE$) and considering different data sequences. Therefore, the achievable performances were verified by considering the benchmark simulator and the Monte–Carlo tool developed in the Matlab® environment. With

these remarks, Table 3 summarises the nominal values of the considered benchmark model simulator parameters with reference to realistic uncertainty values. In fact, the Monte–Carlo analysis has been defined by describing the reliabilities (errors) of the benchmark model parameters as Gaussian stochastic variables, with zero–mean and standard deviations with values as reported in Table 3.

Table 3. Wind farm parameter simulated accuracy for the Monte–Carlo analysis.

Model Variable	Nominal Value & Accuracy (Error)
ρ	1.225 kg/m^3 ± 20%
J	7.794×10^6 kg/m^2 ± 30%
C_p	$C_{p\,0}$ ± 50%
u	u_0 ± 20%
y	y_0 ± 20%

Table 3 also considers that the input–output signals u and y and the entries of the power coefficient C_p–map are affected by error terms described as per–cent standard deviations of the corresponding nominal values u_0, y_0, and $C_{p\,0}$.

On the basis of the simulated parameter uncertainty, the verification of the control scheme performances relies on the average values of the $NSSE\%$ index that is experimentally evaluated with 500 Monte–Carlo runs. This $NSSE\%$ index is evaluated for different combinations of the model parameter as described in Table 3.

Note that Table 3 summarises the parameter accuracy that are considered for analysing the robustness and the reliability features of the developed sustainable control scheme with reference to these parameter changes. In fact, the proposed disturbance decoupling methodology was considered for cancelling out the wind uncertainty and the wind wake effects, and not for taking into account the parameter changes of Table 3.

Table 4 reports the simulation results achieved via the developed Sustainable Control Method (SCM) that includes the baseline wind turbine farm controller with respect to the fault scenario. This approach considers the decoupling of both the wind and the wake effects. Moreover, Table 4 compares the results from other 2 different methodologies, and in particular the Active FTC only with the Wind Decoupling (AFTCWD), and the Passive FTC approach relying on Fuzzy Logic (PFTCFL) (Simani and Farsoni (2018)).

Table 4. Comparison of different FTC performances with respect to the $NSSE\%$ index and the fault cases.

Fault Case	FTC Method SMC	AFTCWD	PFTCFL
1	11.45%	15.33%	14.89%
2	12.67%	16.18%	15.46%
3	11.58%	16.45%	16.92%

In more detail, Table 4 reports the $NSSE\%$ performance index values when the parameters of Table 3 vary according to the Monte–Carlo tool. The performances achieved with the methodology described in this work seem in general better than the ones obtained with the AFTCWD scheme presented in (Simani and Castaldi (2014)) with the simpler wind decoupling, and the fuzzy strategy (PFTCFL) presented in (Simani et al. (2018)). Therefore, it means that the scheme developed in this work presents better tracking errors when compared with the other two approaches. Further investigations will consider the analytic assessment of the stability properties for the developed sustainable control design, possibly applied also to real wind turbine installations.

5. CONCLUSION

This work considered the development of a sustainable control strategy applied to a wind farm benchmark. The proposed controller accommodation strategy employed the recursive reconstruction of the fault signals provided by nonlinear adaptive filters. They were obtained by means of differential algebraic tools that allowed to achieve important disturbance decoupling and robustness features. An identification scheme from input–output data was also exploited for deriving the mathematical description of the nonlinear disturbance distribution functions, which were necessary for the development of the nonlinear adaptive filters for fault reconstruction. These aspects represent key points when recursive applications are proposed for a viable and practical implementation of the suggested sustainable control strategy. A realistic wind park simulated model was used to assess the reliability and robustness features of the proposed methodologies, in the presence of model–reality mismatch effects. Finally, further studies will consider the analysis of the proposed methods when applied to real installations, as well as their mathematical stability and reliability characteristics.

REFERENCES

Castaldi, P., Geri, W., Bonfè, M., Simani, S., and Benini, M. (2010). Design of residual generators and adaptive filters for the FDI of aircraft model sensors. *Control Engineering Practice*, 18(5), 449–459. ACA'07 – 17th IFAC Symposium on Automatic Control in Aerospace Special Issue. Publisher: Elsevier Science. ISSN: 0967–0661. DOI: 10.1016/j.conengprac.2008.11.006.

Castaldi, P., Mimmo, N., and Simani, S. (2014). Differential Geometry Based Active Fault Tolerant Control for Aircraft. *Control Engineering Practice*, 32, 227–235. Invited Paper. DOI:10.1016/j.conengprac.2013.12.011.

Castaldi, P., Mimmo, N., and Simani, S. (2017). Avionic Air Data Sensors Fault Detection and Isolation by means of Singular Perturbation and Geometric Approach. *Sensors*, 17(10), 1–19. Invited paper for the special issue "Models, Systems and Applications for Sensors in Cyber Physical Systems". DOI: 10.3390/s17102202.

Odgaard, P.F. and Stoustrup, J. (2012). Fault Tolerant Control of Wind Turbines using Unknown Input Observers. In C. Verde, C.M. Astorga Zaragoza, and A. Molina (eds.), *Proceedings of the 8th IFAC Symposium on Fault Detection, Supervision and Safety of Technical Processes – SAFEPROCESS 2012*, volume 8, 313–319. National Autonomous University of Mexico, Mexico City, Mexico. DOI: 10.3182/20120829-3-MX-2028.00010.

Odgaard, P.F., Stoustrup, J., and Kinnaert, M. (2013). Fault–Tolerant Control of Wind Turbines: A Benchmark Model. *IEEE Transactions on Control Systems*

Technology, 21(4), 1168–1182. ISSN: 1063–6536. DOI: 10.1109/TCST.2013.2259235.

Odgaard, P.F. and Stoustrup, J. (2013). Fault Tolerant Wind Farm Control – a Benchmark Model. In *Proceedings of the IEEE Multiconference on Systems and Control – MSC2013*, 1–6. Hyderabad, India.

Simani, S. and Castaldi, P. (2017). Robust Control Examples Applied to a Wind Turbine Simulated Model. *Applied Sciences*, 8(29), 1–28. DOI: 10.3390/app8010029. Invited paper for the special issue "Renewable Energy 2018".

Simani, S. and Castaldi, P. (2018). Adaptive Robust Control and its Applications. In A.T. Le (ed.), *Robust Control Applications to a Wind Turbine Simulated System*, chapter 11, 217–233. InTech, Rijeka, Croatia. ISBN: 978-953-51-5729-8. DOI: 10.5772/intechopen.71526.

Simani, S., Fantuzzi, C., and Patton, R.J. (2003). *Model-based fault diagnosis in dynamic systems using identification techniques*, volume 1 of *Advances in Industrial Control*. Springer–Verlag, London, UK, first edition. ISBN: 1852336854.

Simani, S. and Farsoni, S. (2018). *Fault Diagnosis and Sustainable Control of Wind Turbines: Robust data–driven and model–based strategies*. Mechanical Engineering. Butterworth–Heinemann – Elsevier, Oxford (UK), 1st edition. ISBN: 9780128129845.

Simani, S., Farsoni, S., and Castaldi, P. (2018). Data–Driven Techniques for the Fault Diagnosis of a Wind Turbine Benchmark. *International Journal of Applied Mathematics and Computer Science – AMCS*, 28(2), 1–13.

Simani, S. and Castaldi, P. (2014). Active Actuator Fault Tolerant Control of a Wind Turbine Benchmark Model. *International Journal of Robust and Nonlinear Control*, 24(8–9), 1283–1303. John Wiley. DOI: 10.1002/rnc.2993.